Published in final edited form as:
Cancer Biother Radiopharm. 2008 August ; 23(4): 411–423. doi:10.1089/cbr.2007.0450.

Tumor Targeting by a Multivalent Single-Chain Fv (scFv) Anti-Lewis Y Antibody Construct

Marcus P. Kelly[1], **F.-T. Lee**[1], **Kiki Tahtis**[1], **Barbara E. Power**[2], **Fiona E. Smyth**[1], **Martin W. Brechbiel**[3], **Peter J. Hudson**[2], and **Andrew M. Scott**[1]

1*Tumour Targeting Program, Ludwig Institute for Cancer Research, Austin Hospital, Heidelberg, Victoria, Australia*

2*CSIRO Molecular and Health Technologies, Parkville, Victoria, Australia*

3*Radioimmune & Inorganic Chemistry Section, Radiation Oncology Branch, National Cancer Institute, National Institutes of Health, Bethesda, MD*

Abstract

The use of single-chain variable fragment (scFv) constructs has been investigated in cancer radioimmunotherapy (RIT) and radioimmunodetection, as these molecules permit rapid tumor penetration and clearance from the serum relative to whole IgG. Multimerization of scFv constructs has demonstrated improvements in functional affinity (i.e., avidity) and maximal tumor uptake. In this paper, we report the first biodistribution and pharmacokinetics studies of a noncovalent, direct-linked scFv (V_L-0-V_H) trimeric/tetrameric "multimer" of the anti-Lewis Y monoclonal antibody, hu3S193. The in vitro binding and in vivo biodistribution of the hu3S193 multimer was characterized alongside the hu3S193 F(ab′)$_2$ following radiolabeling with the Indium-111 (^{111}In) radioisotope. Immunoreactivities of the radiolabeled multimer and F(ab′)$_2$ were 73% and 53.2%, and binding affinities (K_a) were 1.58×10^7 M^{-1} and 4.31×10^6 M^{-1} for the multimer and F(ab′)$_2$, respectively. Maximal tumor uptake in Le^y -positive MCF-7 breast cancer xenografted BALB/c nude mice was 12.6 ± 2.5 percent injected dose/per gram (%ID/g) at 6 hours postinjection for the multimer and 15.7 ± 2.1 %ID/g at 24 hours postinjection for the F(ab′)$_2$. However, limited in vitro stability and high renal localization of radiolabeled constructs were observed, which, despite the observed tumor targeting of the hu3S193 multimer, most likely preclude its use in RIT and imaging modalities.

Keywords

scFv multimeric construct; hu3S193; biodistribution; Lewis Y antigen

INTRODUCTION

Monoclonal antibodies (mAbs) have emerged as an important new class of therapeutic, with 17 approved Abs currently in clinical use, and over 100 in clinical trials for various applications in the treatment of cancer, inflammatory diseases, and other disorders.[1,2] The specificity of Abs can be especially exploited in cancer, as the expression of tumor-associated antigens on malignancies has allowed the direct targeting of tumors, while avoiding normal tissues lacking expression of the target antigen.[1] Further, Abs can be used as tumor-targeting delivery vehicles

Address correspondence to: Andrew M. Scott; Tumour Targeting Program, Ludwig Institute for Cancer Research, Melbourne Centre for Clinical Sciences, Austin Hospital; 145-163 Studley Road, Heidelberg, Victoria 3084, Australia; Tel.: (613) 9496-5876; Fax: (613) 9496-5892 E-mail: andrew.scott@ludwig.edu.au.

or immunoconjugates for a number of cytotoxic agents, including radioisotopes, chemotherapies, and toxins.[3,4]

A variety of antigens have now been investigated as targets for the mAb therapy of cancer, including the carbohydrate type 2 blood-group-related antigen, Lewis Y,[5] which is overexpressed on tumor cells either as glycolipid or cellsurface glycoproteins.[6] The Le^y antigen has demonstrated expression in up to 60%-90% of tumors and metastases of epithelial origin, including breast, colon, prostate, non-small-cell lung, ovarian, and stomach cancers, presenting it as an attractive target for mAb therapy.[7] The murine anti-Le^y 3S193 Ab was humanized by complimentary-determining region (CDR) grafting the mouse loops residues onto the human REI (V_H) and KOL (V_L) domain frameworks to reduce clinical immunogenicity, and is currently undergoing phase I/II clinical trials in patients with Le^y positive cancers.[8,9] The specificity of hu3S193 make it an attractive candidate for radioimmunotherapy (RIT) of cancer, and the biodistribution and antitumor efficacy of radiolabeled hu3S193 have been investigated in preclinical RIT animal model studies.[6,10]

Although RIT has been proven successful in the treatment of haematologic malignancies, the treatment of solid tumors, such as breast cancer, has proven more difficult, with a number of factors, such as the reduced radiosensitivity of solid tumors, limiting therapeutic efficacy.[11] Particular limitations of RIT include bone marrow toxicity resulting from the long-circulating half-life of radiolabeled mAbs, as well as the heterogenous penetration and irradiation of tumors.[12] Similar issues have arisen when drugs and toxins have been conjugated to Abs in cancer therapy.[4] In an effort to overcome the limitations associated with intact mAbs, genetic engineering has been employed for the modification of Abs and the production of a wide array of antibody fragments, such as Fab and scFv (single-chain variable fragment).[13-16] The most widely used Ab fragment is the scFv, which is produced by joining the genes for the variable heavy and light chain domains with a short oligonucleotide linker between the respective domains to prevent dissociation.[17,18] The reduced size and lack of Fc domian of scFv antibody constructs results in faster pharmacokinetics and potentially more homogenous tumor penetration relative to large IgG molecules.[19] Despite the potential advantages over whole IgG, the use of monovalent scFv has been limited, as total tumor uptake of Ab constructs is low (~3%-5% injected dose per gram [%ID/g]), and high renal accumulation occurs, which may result in both immediate and long-term kidney damage in high-dose applications such as RIT.[3,13,18]

To address the limitations associated with monovalent fragment constructs such as renal accumulation and low affinity, the construction of multivalent scFv constructs has been explored and have appeared to result in increased functional affinities and total tumor uptakes, compared to monovalent scFv molecules.[16,20] Several strategies have been employed to produce multivalent Ab constructs, the most successful being through the reduction in the scFv linker to between zero and five residues, which results in the formation of bivalent dimers (60 kDa), trivalent trimers (80 kDa), or tetravalent tetrabodies (120 kDa).[16,21-24] Single monovalent scFv can be also be covalently linked, with tetravalent scFv produced by noncovalent association of two scFv dimers.[25] Multivalent scFv constructs in the molecular weight range of 60-120 kDa have shown superior avidity and tumor-targeting properties and present as the ideal compromise between rapid pharmacokinetics and sufficient tumor accumulation required in applications such as RIT.[2,14,18]

The biodistribution and tumor-uptake properties of a bivalent 5 residue linker hu3S193 scFv “diabody” have previously been characterized, where specific tumor-targeting and rapid pharmacokinetics demonstrated the promise of hu3S193 scFv constructs.[23] The construction of multivalent engineered constructs, such as the tetrameric hu3S193 V_L-0-V_H scFv multimer (Fig. 1), offers the prospect of improved avidity and tumor uptake while retaining the favorable

pharmacokinetic profile of bivalent scFv constructs, in comparison to whole immunoglobulins. This study is the first to assess the *in vitro* binding properties and *in vivo* biodistribution properties of a novel trimeric/tetrameric V_L-0-V_H scFv multimer and may provide important insights into the potential application of these constructs in the imaging and therapy of cancer.

MATERIALS AND METHODS

Cell Lines

MCF-7, a Le^y-positive breast adenocarcinoma cell line obtained from the American Type Culture Collection (ATCC; Manassas VA) and the colon carcinoma cell line, SW1222 (Ludwig Institute for Cancer Research, New York Branch, New York, NY), were grown in RPMI 1640 media supplemented with 10% fetal calf serum (FCS; CSL Ltd., Vic, Australia) 5% penicillin/streptomycin (Penicillin G 5000 Units/mL/streptomycin sulphate 5000 μg/mL; CSL Ltd., Parksville, Victoria, Australia) and 5% L-glutamine (200 mM stock; JRH Biosciences, Lenexa, KS) in 175-cm^2 flasks (BD Falcon; BD Biosciences, Bedford, MA), and incubated at 37°C in 5% CO_2 incubators (Forma Scientific, Marietta, OH). Cell viability, as determined by trypan blue exclusion, exceeded 90% in all experiments.

Hu3S193 scFv Multimer Production

In the humanized 3S193 V_L-0-V_H scFv multimer gene construct, the V_L domain encodes the residues DIQMTQSPSS. . . . . .GQGTKLQIKR, which are directly linked to the V_H domain encoding the following residues EVQLVESGGG. . . . . .GQGTPVTVSS. The construct contains a C-terminal FLAG affinity purification tail (DYKDDDDK).

The methods used to construct the humanized 3S193 V_L-0-V_H scFv multimer, including the oligonucleotide primers and the method used to assemble the direct linked hu3S193 V_L-0-V_H scFv construct, have been previously described.[21] The method of bacterial expression, using the pPOW vector and subsequent protein purification, have also been previously described.[22] The affinity purified protein from V_L-0-V_H showed, by gel filtration, that the solubilized fraction contained an equilibrium mixture of trimer and tetramer.

Abs and F(ab′)$_2$ Production and Purification

Humanized 3S193 (hu3S193), a CDR-grafted IgG1 antibody specific for the Le^y antigen[9] and isotype control huA33,[26] were produced by the Biological Production Facility, Ludwig Institute for Cancer Research (Melbourne, Vic, Australia). MAbs (10 mg/mL) were used to generate F(ab′)$_2$ fragments by the digestion of the whole Abs using immobilized pepsin (Pierce, Rockford, IL) in a 20-mM sodium acetate buffer (pH 4.5). Digestion was performed overnight in a shaking incubator at 37°C, using an Ab to immobilized pepsin solution ratio of 2:1, as per the manufacturer's instructions. Following digestion, the reaction mixture was neutralized to a pH of 7.5 by the addition of 1.5 mL of Tris-HCl. The F(ab′)$_2$ fragments were initially purified from Fc and undigested IgG by Protein-A affinity chromatography, with additional purification performed by size-exclusion chromatography on a HiLoad™ 16/60 Superdex™ S-200 column (GE Healthcare Biosciences, Uppsala, Sweden). Following purification, the proteins were concentrated by using an Ultracel 50K Amicon Ultra-4 centrifugal filtration device (Millipore Corporation, Billerica, MA) to a final concentration of 3.5 mg/mL for hu3S193 F(ab′)$_2$ and 1.4 mg/mL for huA33 F(ab′)$_2$. The integrity of the purified hu3S193 and huA33 F(ab′)$_2$ fragments was confirmed by sodium dodecyl sulfate polyacrylamide gel electrophoresis (SDS-PAGE) analysis prior to radiolabeling (data not shown).

Chelation and Radiolabeling

Radiolabeling of the multimer and F(ab′)$_2$ constructs with Indium-111 (^{111}InCl; Perkin Elmer Life and Analytical Sciences, Wellesley, MA) was achieved by using the bifunctional metal ion chelate C-functionalized *trans*-cyclohexyldiethylenetriaminepentaacetic acid (CHX-A″-DTPA).[27] Chelation of proteins with CHX-A″-DTPA and subsequent radiolabeling with ^{111}In were performed as outlined in Tahtis et al.[23]

Immunoreactivity and Affinity

Determination of the radiolabeled hu3S193 multimer and F(ab′)$_2$ constructs immunoreactivity was performed according to the "Lindmo" cell-binding assay, using Le^y-positive MCF-7 cells, as previously described.[23] The affinity constant (K_a) and the number of antigen-binding sites per cell were determined by Scatchard analysis.[10,23] The immunoreactivity of the control huA33 F(ab′)$_2$ was determined by a single-point binding assay, where 10×10^6 A33 antigen-positive SW1222 cells were incubated with 20 ng of ^{111}In-CHX-A″-DTPA-huA33-F(ab′)$_2$ for 30 minutes at room temperature. Cells were washed three times, and immunoreactivity was expressed as a percentage of activity in duplicate radioconjugate standards.

Serum Stability

Serum stability of the hu3S193 multimer and hu3S193 and huA33 F(ab′)$_2$ constructs was assessed by incubating each construct (2 μg protein) in 200 μL of healthy donor human serum at 37°C over a 24-hour period, given the expected short half-life *in vivo*.[23] The radiochemical purity of the sample was assessed at 0, 2, 4, and 24 hours by instant thin-layer chromatography (ITLC),[28] as previously described.[10] Single-point immunoreactivity assays were also performed at each time point, where 20 ng of the incubated radiolabeled constructs was added to 50×10^6 MCF-7 or 10×10^6 SW1222 cells, as required, and incubated for 30 minutes at room temperature. As detailed above, the cells were washed, and the percentage of immunoreactivity was determined against the standards.

Chromatographic Analysis

Radiolabeled constructs were analyzed by fast protein liquid chromatography (FPLC) immediately following radiolabeling, using the method previously described to assess the integrity of the proteins.[23] The integrity of the proteins were also analyzed by size-exclusion chromatography following incubation in normal human serum for 2 hours at 37°C. Following incubation, the proteins were separated on a HiLoad™ 16/60 Superdex™ S-200 column (GE Healthcare Biosciences) and collected as 60 22-minute fractions, using a RediFrac fraction collector (GE Healthcare Biosciences). Protein in the fractions was determined by ultraviolet (UV) absorbance at 280 nm, using a DU530 UV spectrophotometer (Beckman Instruments, Fullerton, CA), and radioactivity was measured in a dual gamma counter (Cobra™ II Auto-Gamma; Packard Instruments, Canberra, Australia).

Xenograft Model

Tumor xenografts were established in 3-4-week-old female BALB/c nude mice obtained from the Animal Resource Centre, Perth WA, Western Australia. MCF-7 breast carcinoma xenografts were established by injecting 20×10^6 MCF-7 cells into the left mammary line of BALB/c nude mice. Prior to the injection of the cells, the animals were implanted with a slow-release estrogen pellet to sustain the osteogen-dependent MCF-7 cells, as previously described.[10] The Le^y-negative SW1222 control xenografts were established on the opposite flank to the principle MCF-7 tumor, as previously described.[6] Tumor growth was measured by using digital calipers, as well as the formula: Tumor Volume = (length × width^2)/2 of the tumor, and expressed in cubic millimeters.

Biodistribution Study

The biodistribution of the ^{111}In-radiolabeled multimer and F(ab′)$_2$ constructs was assessed in two separate studies. In the hu3S193 multimer study, 55 mice (MCF-7 tumor volume, 362.0 ± 66.4 mm^3) were injected with the ^{111}In-multimer (3.3 μg, protein, 1.86 μCi) by tail vein injection. Following radiolabeling, the hu3S193 multimer was purified by FPLC before injection into the mice. Groups of 5 mice were culled at 10 and 30 minutes and at 1, 2, 4, 6, 8, 24, 48, 72, and 120 hours after the injection of the radioconjugate. At each time point, the mice were euthanized by isofluorane anesthesia and then immediately bled via cardiac puncture. Tumors and normal tissues (e.g., liver, spleen, kidney, muscle, skin, bone, lung, heart, stomach, brain, small bowel, and tail) were then resected, placed in individual γ-counter tubes, and weighed. The activity of all samples was then counted on a dual gamma scintillation counter (Cobra II Auto Gamma; Packard Instruments), and the %ID/g was calculated. Results were expressed as the mean ± standard deviation for each time point, and used in the calculation of tumor:blood (T:B) ratios.

To assess the biodistribution of the F(ab′)$_2$ constructs, 50 mice (MCF-7 tumor volume = 411.5 ± 89.1 mm^3) were injected with either^{111}In-hu3S193 F(ab′)$_2$ (4.5 μg, 10.6 μCi) or^{111}In-huA33 F(ab′)$_2$ (4.5 μg, 11.6 μCi). Groups of 4 (hu3S193) or 3 mice (huA33) were then culled at 10 minutes and at 1, 2, 6, 8, 24, and 72 hours after the injection of the radioconjugate, and the % ID/g for each time point was determined in the tumor and normal tissues, as outlined for the multimer studies.

Gamma-Camera Imaging

Whole-body imaging of a mouse was performed to identify tumor localization of the radiolabeled construct 24 hours after the radioconjugate injection. Mice were anesthetized with a mixture of 20 mg/kg of xylazine/100 mg/kg ketamine (10 μL/g) by an intraperitoneal injection and placed under a Philips Axis gamma camera (Phillips Medical Systems, North Ryde, Australia). Images of 20,000 counts were acquired at each time point, using a 128 × 128 matrix, and a zoom of 2. A standard equivalent to 10%ID was included in the field of view.

Pharmacokinetic and Area Under the Curve (AUC) Analysis

The pharmacokinetics ($T_{½}\alpha$ and $T_{½}\beta$) of the hu3S193 multimer construct was calculated by using the serum clearance data from the biodistribution study. A two-compartment intravenous-bolus model with a first-order elimination was fitted to the data by using the WinNonLin curve-fitting program (WinNonLin Pro Node 5.0.1; Pharsight Co., Mountain View, CA). Area under the curve (AUC) ratios were calculated by the integration of the serum clearance and MCF-7 tumor uptake curves of the respective constructs investigated, using GraphPad Prism (version 4; GraphPad Software, Inc., La Jolla, CA) and dividing the MCF-7 area by the serum clearance area.

RESULTS

Immunoreactivity and Affinity Analysis

The immunoreactivity of the ^{111}In-labeled multimer was 73%. Immunoreactivity of the hu3S193 F(ab′)$_2$ was lower, when compared to the multimer construct, at 53.2%, although this was comparable to previous determinations of hu3S193 F(ab′)$_2$ immunoreactivity.[23] Affinity of the hu3S193 multimer was 1.58×10^7 M^{-1}, which is slightly higher, compared to the previously reported affinity of the intact hu3S193 mAb.[6,10] In contrast, the affinity of the hu3S193 F(ab′)$_2$ of 4.31×10^6 M^{-1} was around 10-fold lower than the multimer construct, although still equivalent to previous determinations of intact hu3S193 and F(ab′)$_2$ affinities.[9,23]

Serum-Stability Analysis

The results of serum stability of the radiolabeled constructs over 24 hours are shown in Table 1. No significant loss of immunoreactivity was observed with the hu3S193 multimer construct following the 2-hour incubation, with radiochemical purity also stable. These results correlate with the chromatographic analysis of the multimer following radiolabeling (Fig. 2A) and the 2-hour serum incubation (Fig. 2B). Following radiolabeling, the trimer-tetramer multimer was observed as two distinct radiolabeled constructs eluting at the expected fraction. Some labeling of a high-molecular-weight aggregate is observed, as was the formation of unlabeled low-molecular-weight constructs (monomeric or dimeric hu3S193 scFv). After serum incubation for 2 hours, most activity was still associated with the multimer construct (Fig. 2B), although increased formation of the high-molecular-weight aggregates was more apparent. The single peak present in Figure 2B most likely indicates a less sensitive separation of the trimer-tetramer multimer by column chromatography relative to FPLC analysis used directly following radiolabeling, and not the breakdown of the trimeric scFv. However, the conversion of trimeric scFv to higher molecular weight forms may also explain the appearance of a single peak. No low-molecular-weight constructs were observed at this time. From the 4-hour incubation, a 7-fold reduction in immunoreactivity occurred. Radiochemical purity did not undergo this deterioration and remained above 90% for the duration of the incubation period.

The hu3S193 $F(ab')_2$ constructs demonstrated greater stability relative to the multimer construct: Only a moderate reduction in immunoreactivity of ~10% occurred over the 24-hour incubation period, with radiochemical purity remaining above 95%. Chromatographic analyses confirmed this stability, with the radiolabeled $F(ab')_2$ eluting as a single peak in the expected fraction at both times investigated (Fig. 2C and 2D). The isotype control huA33 $F(ab')_2$ retained stability and demonstrated no real change in immunoreactivity following the serum incubation.

Biodistribution of Constructs

Uptake to Le^y-positive MCF-7 tumors was observed with both the hu3S193 multimer and $F(ab')_2$. Average MCF-7 tumor volume was 362 ± 66 mm^3 for the hu3S193 multimer study and 411 ± 89 mm^3 for the hu3S193 $F(ab')_2$ study. Maximal tumor uptake of ^{111}In-labeled multimer was 12.6 ± 2.5%ID/g at 6 hour postinjection (Figure 3A), contrasting with maximal uptake of the ^{111}In-labeled hu3S193 $F(ab')_2$ of 15.7 ± 2.1%ID/g, which was observed at 24 hours postinjection (Fig. 3B). Uptake of both constructs in the Le^y-negative SW1222 control tumors was negligible, and was not observed to increase with time, as was observed in MCF-7 tumors (Fig. 3C and 3D). As shown in Figure 3A and 3B, both constructs demonstrated high %ID/g in the kidneys. Additionally, significant uptake was observed in the liver, although it is likely that this was associated with the known catabolism and sequestration of ^{111}In-radiolabeled complexes by the reticuloendothelial system, rather than specific targeting of the liver by the anti-Le^y constructs.[10] No other significant or sustained localization was observed in the other normal tissues investigated. Following injection, the hu3S193 multimer demonstrated a rapid distribution phase ($T_{½}\alpha$, 1.80 hour), with an overall clearance rate of 987 mL/hour. The hu3S193 $F(ab')_2$ displayed a slightly slower equilibration phase ($T_{½}$, 2.42 hours), and an overall clearance rate of 359 mL/hour.

Quantitative Tumor Uptake and Blood Clearance

T:B ratios were calculated from the %ID/g values that were calculated from the *in vivo* biodistribution study (Table 2). Values obtained from the previous *in vivo* characterization of the hu3S193 dimeric scFv "diabody" construct are included for comparison. The hu3S193 multimer construct demonstrated the highest T:B ratio of 57:1 at the time points investigated (5.3 vs. 0.09 %ID/g at 72 hours postinjection), although the ratios for the diabody were generally comparable and were superior at most time points. The T:B ratios for the hu3S193

$F(ab')_2$ construct were much lower (15.6:1; 8.45 vs. 0.54 %ID/g at 72 hours postinjection), compared to either the diabody or multimer, most likely due to its slower pharmacokinetics.

AUC comparisons support the T:B ratio analysis. A tumor AUC of 611.2 was calculated for the hu3S193 multimer and was greater than the diabody tumor AUC of 146.3. The diabody AUC for blood clearance was similarly reduced relative to the multimer (23.1 vs. 97.3), resulting in the respective scFv constructs demonstrating similar T:B AUC ratios. Again, as the hu3S193 $F(ab')_2$ construct maintained higher serum levels compared to the scFv constructs, its T:B AUC ratio was, accordingly, half that of the other constructs.

In Vivo Gamma-Camera Imaging

Gamma-camera imaging of a mouse injected with the radiolabeled multimer was undertaken to further assess their *in vivo* localization to tumor and normal tissues. The tumor volume of the imaged MCF-7 xenograft was 416 mm^3. Images were obtained 24 hours postinjection, as shown in Figure 4. Renal accumulation of the multimer is particularly evident. Specific MCF-7 tumor localization is apparent (white arrow). No specific uptake of the anti-Le^y constructs was observed in the Le^y-negative control SW1222 tumors. In mice injected with control huA33 $F(ab')_2$, no localization to MCF-7 tumors was apparent, although uptake into A33 antigen-positive SW1222 tumors was observed (data not shown).

DISCUSSION

The use of mAbs to selectively target tumors through tumor-associated antigens offers an alternative avenue of cancer therapy, as well as a means to selectively target a variety of cytotoxic agents, such as radioisotopes, drugs, toxins, or enzymes, directly to tumor cells.[15] In the treatment of solid tumors with modalities such as RIT, a number of impediments to successful treatment are apparent, such as limited tumor vascularization, heterogenous tumor penetration of antibody, and long serum half-lives of IgG, which results in the exposure of normal tissues to radioactivity.[14] In an effort to overcome these obstacles, the use of smaller enzymatically produced Fab fragments and genetically engineered scFv constructs with more favorable pharmacokinetic profiles have been investigated.[15] Further engineering of scFv constructs can lead to the production of high-avidity multivalent constructs and an array of associated antibody-like reagents.[2] The aim of this study was to evaluate the potential of a radiolabeled scFv trimeric/tetrameric multimer (90-120 kDa) of anti-Le^y mAb hu3S193 for eventual use as an imaging or therapeutic reagent in Le^y-expressing cancers.[21]

Both the hu3S193 scFv multimer and $F(ab')_2$ construct were radiolabeled successfully with the ^{111}In radioisotope through the use of the CHX-A″-DTPA chelate. The hu3S193 multimer demonstrated high immunoreactivity (73%), which is superior to the 41.3% determined for the hu3S193 diabody and other values previously obtained for hu3S193 IgG.[10,23] Further, the affinity of the multimer construct, as determined by Scatchard analysis, was slightly better than previously observed for hu3S193 IgG and around 10-fold higher than observed for the hu3S193 $F(ab')_2$ and diabody, respectively. It is likely that the improved immunoreactivity and apparent functional affinity (i.e., avidity) of the hu3S193 multimer over the diabody are a direct result of increased valency. Similar increases in avidity have been observed following the multimerization of other monomeric and dimeric scFv molecules.[14,16] Despite improved immunoreactivity and avidity observed with the hu3S193 multimer, it is apparent that the serum stability of the construct is limited. Decreased immunoreactivity and formation of high-molecular-weight aggregates was observed following the incubation of the hu3S193 multimer at 37°C, indicating a possible dissociation of the noncovalently bound scFv fragments. The hu3S193 $F(ab')_2$ construct and isotype control huA33 $F(ab')_2$ demonstrated excellent serum stability, indicating that these molecules retain the relative inherent serum stability of the parental IgG.

The hu3S193 multimer demonstrated rapid pharmacokinetics, compared to previously determined values for intact hu3S193 IgG (multimer $T_{½}\alpha$, 1.8 hours vs. IgG $T_{½}\alpha$, 7.4 hours), and had completely cleared from the blood within 24 hours. Multimer specifically targeted Le^y-positive MCF-7 tumor, with a peak uptake of 12.6 ± 2.5 %ID/g apparent at 6 hours postinjection. Importantly, the specific targeting of the hu3S193 multimer to tumor was also observed by gamma-camera imaging. To date, the only other extensively characterized tetravalent scFv construct targeting solid tumor is the tetrameric CC49 scFv $[scFv_2]_2$ construct targeting the glycoprotein tumor-associated antigen, TAG-72, which is expressed on a broad range of human adenocarcinomas.[15,19,25] In a study comparing divalent and tetravalent forms of CC49 scFv radiolabeled with ^{99m}Tc, LS174T colon tumor localization of the tetravalent $[scFv_2]_2$ reached a peak of 19.1 ± 1.1 %ID/g at 6 hours postinjection, compared to 7.2 ± 0.7 %ID/g for divalent $scFv_2$.[20] In further studies with scFv CC49 constructs using other radioisotopes, including ^{125}I, ^{131}I, and ^{177}Lu, improved biodistribution and tumor localization (~2-fold) were consistently observed with tetrameric constructs over dimeric equivalents.[15, 19,25,29] The hu3S193 multimer in the current study reached tumor uptake levels approaching that of tetravalent $[scFv_2]_2$ CC49, although direct comparison is complicated by the different structures of the respective tetravalent molecules and the tumor models used to investigate their biodistribution.

As observed in the studies of scFv CC49 and other constructs, an increase in tumor localization was observed in the current study with the hu3S193 multimer, compared to the previously characterized diabody construct.[15,21,23,24] Our previous characterization of scFv the hu3S193 diabody demonstrated maximal tumor localization of 4.7 ± 0.6 %ID/g at 1 hour postinjection, with a maximal tumor-to-blood ratio of 40:1 observed at 8 hours postinjection. In comparison, the maximal uptake of the hu3S193 multimer at 6 hours postinjection was nearly 3-fold greater at 12.6 ± 2.5 %ID/g. However, when the ratio of tumor localization to blood exposure is compared though calculating AUC ratios for the respective constructs, little difference was observed, with multimer AUC ratio of 6.28:1 versus 6.32:1 for the diabody. From these analyses, it is apparent that use of the hu3S193 multimer permits higher tumor localization than the diabody but with little change in the overall T:B ratios. Importantly, although hu3S193 $F(ab')_2$ was observed to have a higher absolute tumor uptake of 15.7 ′ 2.2 %ID/g relative to the multimer, a slower clearance resulted in inferior T:B rations.

From the biodistribution studies and as clearly apparent in gamma-camera images (Fig. 4), the hu3S193 multimer and demonstrated significant localization to the kidneys due to clearance though glomerular filtration and the retention of radiometal metabolites in the renal system.[15,30,31] The limited *in vitro* stability of the hu3S193 multimer, rapid pharmacokinetics, and high renal uptake suggest that at low concentration *in vivo*, the construct may dissociate into monomeric scFvs, as previously observed in studies of 15-9 scFv diabody targeting laminin-1.[32] However, higher renal retention than that of the multimer was observed for the hu3S193 $F(ab')_2$, indicating the likely cleavage of $F(ab')_2$ into smaller Fab′ fragments by the reduction of disulfide links and their subsequent elimination by the kidneys.[33] Further, this result indicates that the apparent superiority of $F(ab')_2$ serum stability over the multimer *in vitro* is not retained *in vivo*. Such rapid, significant renal localization by the constructs is of concern, as the retention of radiometals results in renal toxicity that limits the clinical application of scFvs constructs in RIT and radioimmunoimaging.[34,35] The coadministration of cationic amino acids, such as L-lysine, has been observed to greatly reduce the renal retention of antibody fragments and could be used with the hu3S193 multimer to prevent the significant renal uptake observed in these studies.[15,35-38] However, the administration of such amino acids does not always significantly alter the renal uptake of fragments and does not improve the total tumor accumulation of the target constructs.[34,37] With respect to liver loading and processing, both the scFv multimers in our study and the tri- and tetrameric scFv constructs of others[14,16] exhibit the expected liver uptake that is not dependent on the Fc-mediated

internalization pathway inherent to intact antibodies or scFv-Fc fusions engaging the neonatal Fc-receptor.[39] Indeed, one tetrameric antibody format that retained Fc-mediated interactions possessed both improved pharmacokinetics and *in vitro* cytotoxicity, compared to the bivalent formulation.[40]

The low stability observed of the multimer, and the resultant high renal retention of scFv fragments, requires efforts to improve the overall stability of the multimer, which, in turn, may lead to more prolonged tumor localization than currently experienced. The stability of the hu3S193 multimer is dependent on the affinity of the interaction of the individual V_H and V_L domains to associate into each Fv, and efforts to increase the affinity of this interaction may improve the stability of the complete multimer.[21] Indeed, Fv fragments have a wide range of stabilities that are dependent on the enthalpic and entropic parameters that result from close association of V_H and V_L domain pairs. Practically, some antibody Fv fragments exhibit remarkable stability, whereas others are unstable, in loose association, that cannot be improved, even by fusion to Constant domains to recreate the parent Fab fragment.[41] For hu3S193, it may be possible to improve Fv stability by (1) mutation and selection of higher stability V-domain interfaces,[42] (2) by selective design of “knobs into holes” mutations to improve interface-binding kinetics.[1] (3) addition of cysteine residues capable of interface (i.e., interdomain) disulphide bond formation,[41] or (4) construction of bis-tetrabodies.[25,43-48] It is also possible to increase stability by fusion to high-affinity protein or peptide pairs, such as the Barnase ribonuclease and Barstar module, which has a dissociation constant of ~10^{-14} M, and was used to construct a stable trimeric scFv anti-$p185^{HER2\text{-}ECD}$ 4D5.[49] High serum stability, increase in tumor localization, and a converse decrease in renal retention were observed upon multimerization, indicating the usefulness of the Barnsase-Barstar system in this case and its application to other scFv multimers.

The trimeric/tetrameric hu3S193 scFv multimer demonstrated increased avidity and *in vivo* tumor localization over the previously characterized dimeric hu3S193 scFv diabody. Similar effects have been observed with tetramers of covalently linked $sc(Fv)_2$ dimers, although the current study is the first to report such improvements following the change from a five-residue-linked scFv dimer to a zero-linked scFv trimer/tetramer construct.[15]

CONCLUSIONS

These studies provide the first *in vivo* biodistribution and pharmacokinetics characterization of a multimeric scFv construct produced through the noncovalent association of 0-linker variable domains (V_L-0-V_H) and possibly indicates the likely behavior of other constructs produced though this method. It is apparent that the high renal uptake of the multimer and associated breakdown products needs to be addressed by efforts to improve the construct's stability before any further evaluation could proceed. Following intensive optimization and improved tumor targeting, engineered antibody constructs, such as the hu3S193 scFv multimer, may eventually be valuable components in cancer immunotherapy and imaging.

ACKNOWLEDGMENTS

The authors wish to thank Usha Krishnan for protein purification of the hu3S193 multimer and also Angela Rigopoulos, Dongmao Wang, and Sanja Coso for their assistance in the biodistribution study, Anthony Papenfuss for pharmacokinetic calculations, and the staff from the Department of Nuclear Medicine, Austin Hospital, for their assistance in the gamma-camera imaging of the animals. This research was funded by the NH&MRC Program Grant 290816 and, in part, by the Intramural Research Program of the NIH, National Cancer Institute, Center for Cancer Research. MPK was supported by a Melbourne Research Scholarship, University of Melbourne (Melbourne, Australia).

REFERENCES

1. Carter PJ. Potent antibody therapeutics by design. Nat Rev Immunol 2006;6:343. [PubMed: 16622479]
2. Holliger P, Hudson PJ. Engineered antibody fragments and the rise of single domains. Nat Biotechnol 2005;23:1126. [PubMed: 16151406]
3. Sharkey RM, Karacay H, Cardillo TM, et al. Improving the delivery of radionuclides for imaging and therapy of cancer using pretargeting methods. Clin Cancer Res 2005;11:7109s. [PubMed: 16203810]
4. Wu AM, Senter PD. Arming antibodies: Prospects and challenges for immunoconjugates. Nat Biotechnol 2005;23:1137. [PubMed: 16151407]
5. Jostock T, Vanhove M, Brepoels E, et al. Rapid generation of functional human IgG antibodies derived from Fab-on-phage display libraries. J Immunol Meth 2004;289:65.
6. Kelly MP, Lee FT, Smyth FE, et al. Enhanced efficacy of ^{90}Y-radiolabeled anti-Lewis Y humanized monoclonal antibody hu3S193 and paclitaxel combined-modality radioimmunotherapy in a breast cancer model. J Nucl Med 2006;47:716. [PubMed: 16595507]
7. Zhang S, Zhang HS, Cordon-Cardo C, et al. Selection of tumor antigens as targets for immune attack using immunohistochemistry: II. Blood group-related antigens. Int J Cancer 1997;73:50. [PubMed: 9334809]
8. Scott AM, Tebbutt N, Lee F-T, et al. Phase I trial of hu3S193 in patients with advanced epithelial cancers which express the Lewis Y antigen. [Meeting Abstracts] J Clin Oncol 2004;22:2567.
9. Scott AM, Geleick D, Rubira M, et al. Construction, production, and characterization of humanized anti-Lewis Y monoclonal antibody 3S193 for targeted immunotherapy of solid tumors. Cancer Res 2000;60:3254. [PubMed: 10866319]
10. Clarke K, Lee FT, Brechbiel MW, et al. *In vivo* biodistribution of a humanized anti-Lewis Y monoclonal antibody (hu3S193) in MCF-7 xenografted BALB/c nude mice. Cancer Res 2000;60:4804. [PubMed: 10987290]
11. Sharkey RM, Goldenberg DM. Perspectives on cancer therapy with radiolabeled monoclonal antibodies. J Nucl Med 2005;46(Suppl 1):115S. [PubMed: 15653660]
12. Buchsbaum DJ, Rogers BE, Khazaeli MB, et al. Targeting strategies for cancer radiotherapy. Clin Cancer Res 1999;5:3048s. [PubMed: 10541342]
13. Adams GP, Schier R. Generating improved single-chain Fv molecules for tumor targeting. J Immunol Meth 1999;231:249.
14. Batra SK, Jain M, Wittel UA, et al. Pharmacokinetics and biodistribution of genetically engineered antibodies. Curr Opin Biotechnol 2002;13:603. [PubMed: 12482521]
15. Chauhan SC, Jain M, Moore ED, et al. Pharmacokinetics and biodistribution of ^{177}Lu-labeled multivalent single-chain Fv construct of the pancarcinoma monoclonal antibody CC49. Eur J Nucl Med Mol Imaging 2005;32:264. [PubMed: 15791435]
16. Kortt AA, Dolezal O, Power BE, et al. Dimeric and trimeric antibodies: High avidity scFvs for cancer targeting. Biomol Eng 2001;18:95. [PubMed: 11566601]
17. Hudson PJ, Souriau C. Engineered antibodies. Nat Med 2003;9:129. [PubMed: 12514726]
18. Huhalov A, Chester KA. Engineered single-chain antibody fragments for radioimmunotherapy. Q J Nucl Med Mol Imaging 2004;48:279. [PubMed: 15640791]
19. Wittel UA, Jain M, Goel A, et al. The *in vivo* characteristics of genetically engineered divalent and tetravalent single-chain antibody constructs. Nucl Med Biol 2005;32:157. [PubMed: 15721761]
20. Goel A, Baranowska-Kortylewicz J, Hinrichs SH, et al. ^{99m}Tc-labeled divalent and tetravalent CC49 single-chain Fvs: Novel imaging agents for rapid *in vivo* localization of human colon carcinoma. J Nucl Med 2001;42:1519. [PubMed: 11585867]
21. Power BE, Doughty L, Shapira DR, et al. Noncovalent scFv multimers of tumor-targeting anti-Lewis (y) hu3S193 humanized antibody. Protein Sci 2003;12:734. [PubMed: 12649432]
22. Power BE, Hudson PJ. Synthesis of high-avidity antibody fragments (scFv multimers) for cancer imaging. J Immunol Meth 2000;242:193.
23. Tahtis K, Lee FT, Smyth FE, et al. Biodistribution properties of (111)indium-labeled C-functionalized transcyclohexyl diethylenetriaminepentaacetic acid humanized 3S193 diabody and F(ab′)(2)

constructs in a breast carcinoma xenograft model. Clin Cancer Res 2001;7:1061. [PubMed: 11309358]

24. Todorovska A, Roovers RC, Dolezal O, et al. Design and application of diabodies, triabodies, and tetrabodies for cancer targeting. J Immunol Meth 2001;248:47.
25. Goel A, Colcher D, Baranowska-Kortylewicz J, et al. Genetically engineered tetravalent single-chain Fv of the pancarcinoma monoclonal antibody CC49: Improved biodistribution and potential for therapeutic application. Cancer Res 2000;60:6964. [PubMed: 11156397]
26. Scott AM, Lee F-T, Jones R, et al. A phase I trial of humanized monoclonal antibody A33 in patients with colorectal carcinoma: Biodistribution, pharmacokinetics, and quantitative tumor uptake. Clin Cancer Res 2005;11:4810. [PubMed: 16000578]
27. Wu C, Kobayashi H, Sun B, et al. Stereochemical influence on the stability of radio-metal complexes *in vivo*. Synthesis and evaluation of the four stereoisomers of 2-(p-nitrobenzyl)-trans-CyDTPA. Bioorg Med Chem 1997;5:1925. [PubMed: 9370037]
28. Nikula TK, Curcio MJ, Brechbiel MW, et al. A rapid, single-vessel method for preparation of clinical grade ligand conjugated monoclonal antibodies. Nucl Med Biol 1995;22:387. [PubMed: 7627155]
29. Goel A, Augustine S, Baranowska-Kortylewicz J, et al. Single-dose versus fractionated radioimmunotherapy of human colon carcinoma xenografts using ^{131}I-labeled multivalent CC49 single-chain fvs. Clin Cancer Res 2001;7:175. [PubMed: 11205906]
30. Duncan JR, Welch MJ. Intracellular metabolism of indium-111-DTPA-labeled receptor targeted proteins. J Nucl Med 1993;34:1728. [PubMed: 8410290]
31. Press OW, Shan D, Howell-Clark J, et al. Comparative metabolism and retention of iodine-125, yttrium-90, and indium-111 radioimmunoconjugates by cancer cells. Cancer Res 1996;56:2123. [PubMed: 8616860]
32. Huang B-C, Foote LJ, Lankford TK, et al. A diabody that dissociates to monomer forms at low concentration: effects on binding activity and tumor targeting. Biochem Biophys Res Commun 2005;327:999. [PubMed: 15652494]
33. Quadri SM, Siddiqui A, Klein JL, et al. Biodistribution and tumor localization of ^{111}In-labeled unmodified and modified F(ab′)$_2$ fragments of human monoclonal IgM (16.88) in a nude mouse model. Nucl Med Biol 1995;22:413. [PubMed: 7550017]
34. Rutherford RA, Smith A, Waibel R, et al. Differential inhibitory effect of L-lysine on renal accumulation of ^{67}Cu-labelled F(ab′)$_2$ fragments in mice. Int J Cancer 1997;72:522. [PubMed: 9247299]
35. Behr TM, Sharkey RM, Juweid ME, et al. Reduction of the renal uptake of radiolabeled monoclonal antibody fragments by cationic amino acids and their derivatives. Cancer Res 1995;55:3825. [PubMed: 7641200]
36. Arano Y, Fujioka Y, Akizawa H, et al. Chemical design of radiolabeled antibody fragments for low renal radioactivity levels. Cancer Res 1999;59:128. [PubMed: 9892197]
37. Behe M, Kluge G, Becker W, et al. Use of polyglutamic acids to reduce uptake of radiometal-labeled minigastrin in the kidneys. J Nucl Med 2005;46:1012. [PubMed: 15937313]
38. Gansow OA, Brechbiel MW, Mirzadeh S, et al. Chelates and antibodies: Current methods and new directions. Cancer Treat Res 1990;51:153. [PubMed: 1977442]
39. Ferl GZ, Kenanova V, Wu AM, et al. A two-tiered physiologically based model for dually labeled single-chain Fv-Fc antibody fragments. Mol Cancer Ther 2006;5:1550. [PubMed: 16818514]
40. Liu X-Y, Pop LM, Roopenian DC, et al. Generation and characterization of a novel tetravalent anti-CD22 antibody with improved antitumor activity and pharmacokinetics. Int Immunopharmacol 2006;6:791. [PubMed: 16546710]
41. Rothlisberger D, Honegger A, Pluckthun A. Domain interactions in the Fab fragment: A comparative evaluation of the single-chain Fv and Fab format engineered with variable domains of different stability. J Mol Biol 2005;347:773. [PubMed: 15769469]
42. Wark KL, Hudson PJ. Latest technologies for the enhancement of antibody affinity. Adv Drug Del Rev 2006;58:657.
43. Brinkmann U, Di Carlo A, Vasmatzis G, et al. Stabilization of a recombinant Fv fragment bybase-loop interconnection and VH-VL permutation. J Mol Biol 1997;268:107. [PubMed: 9149145]

44. Dall'Acqua W, Carter P. Antibody engineering. Curr Opin Struct Biol 1998;8:443. [PubMed: 9729735]

45. Le Gall F, Reusch U, Little M, et al. Effect of linker sequences between the antibody variable domains on the formation, stability, and biological activity of a bispecific tandem diabody. Protein Eng Des Sel 2004;17:357. [PubMed: 15126676]

46. Olafsen T, Cheung CW, Yazaki PJ, et al. Covalent disulfide-linked Anti-CEA diabody allows site-specific conjugation and radiolabeling for tumor-targeting applications. Protein Eng Des Sel 2004;17:21. [PubMed: 14985534]

47. Reusch U, Le Gall F, Hensel M, et al. Effect of tetravalent bispecific CD19 × CD3 recombinant antibody construct and CD28 costimulation on lysis of malignant B-cells from patients with chronic lymphocytic leukemia by autologous T cells. Int J Cancer 2004;112:509. [PubMed: 15382079]

48. Zhu Z, Presta LG, Zapata G, et al. Remodeling domain interfaces to enhance heterodimer formation. Protein Sci 1997;6:781. [PubMed: 9098887]

49. Deyev SM, Waibel R, Lebedenko EN, et al. Design of multivalent complexes using the barnase*barstar module. Nat Biotechnol 2003;21:1486. [PubMed: 14634668]

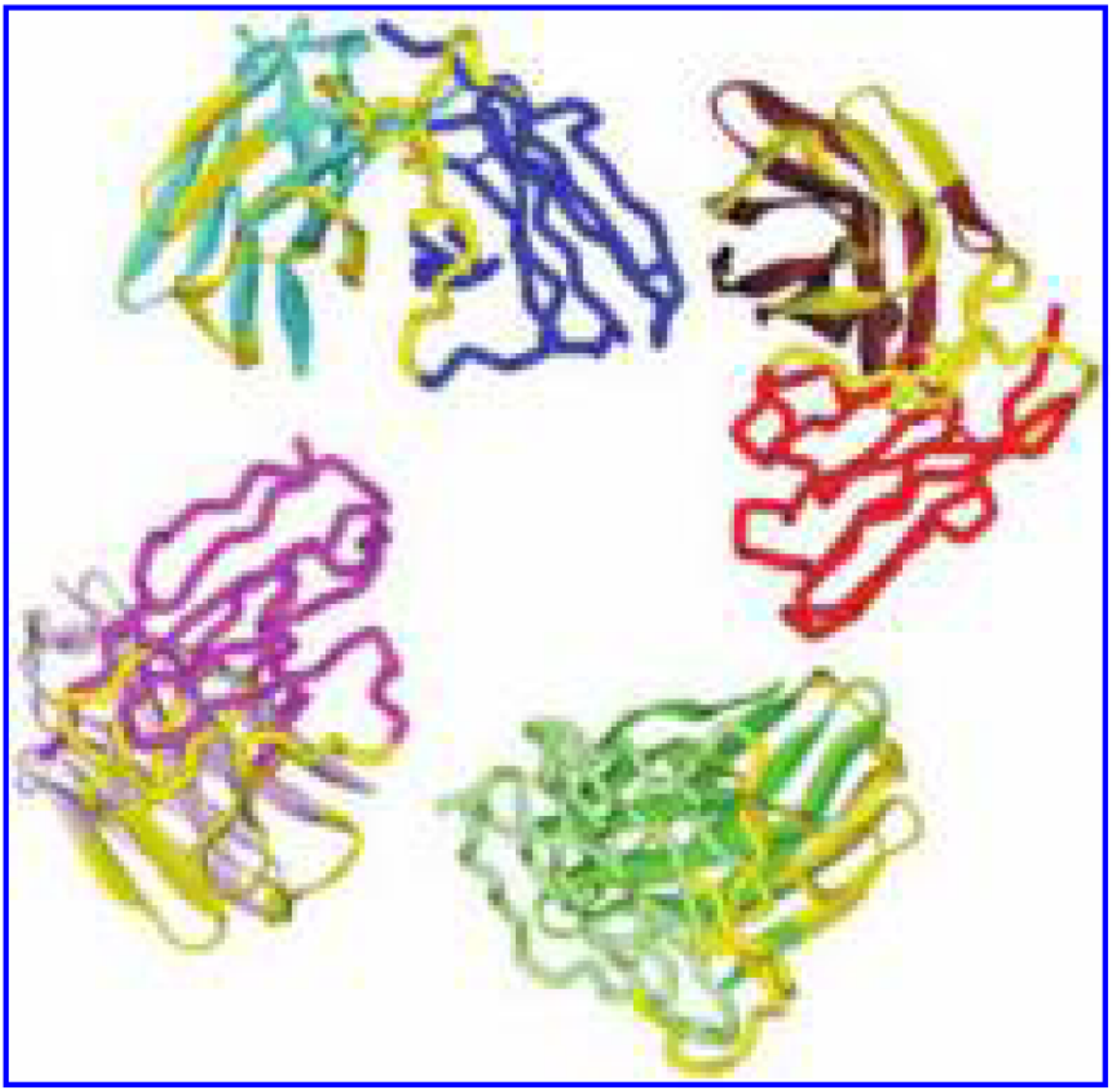

Figure 1.
Model of the 3S193 tetrameric V_L-0-V_H single-chain Fv "multimer" construct. The complementary-determining regions for each binding site are shown in yellow. The V_H domains are depicted as ribbons, and the V_L domains are shown as wires.

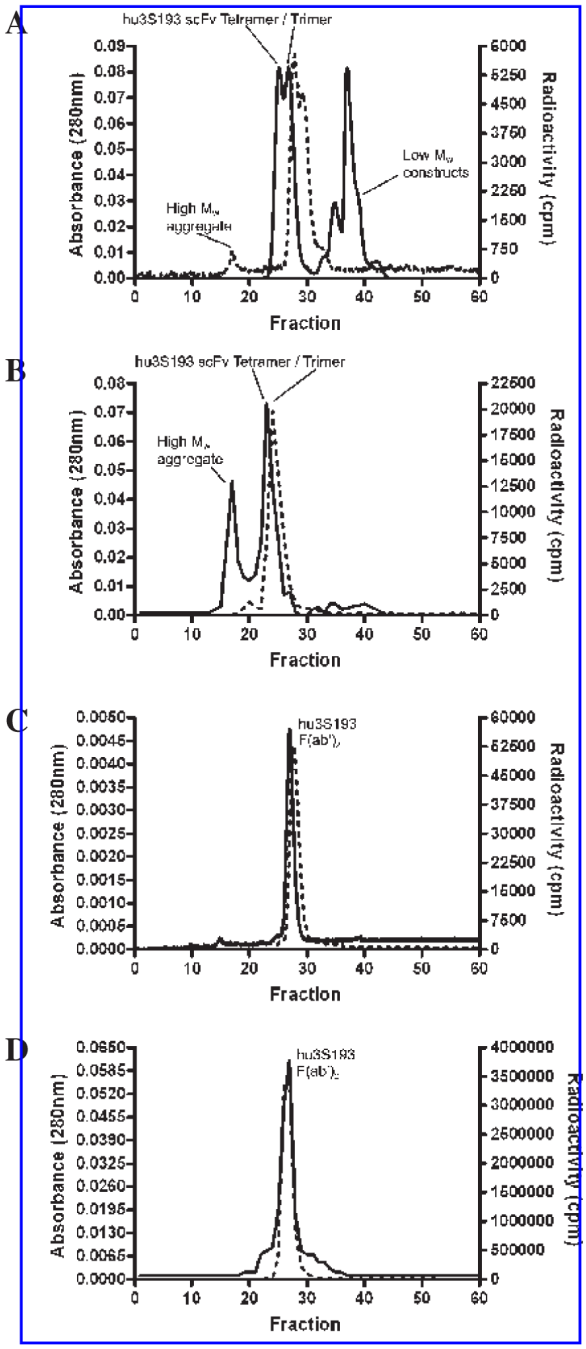

Figure 2.

Analysis of hu3S193 multimer and F(ab′)$_2$ constructs by fast protein liquid chromatography (FPLC) size-exclusion chromatography. Multimer was assessed immediately following radiolabeling by (**A**) FPLC and by (**B**) size-exclusion chromatography following a 2-hour incubation in normal human serum. F(ab′)$_2$ was assessed immediately following radiolabeling by (**C**) FPLC and by (**D**) size-exclusion chromatography following a 2-hour incubation in normal human serum. Protein detected as absorbance at 280 nm (A_{280}) is represented by (—), and radioactivity measured as count per minute (cpm) is represented by (---).

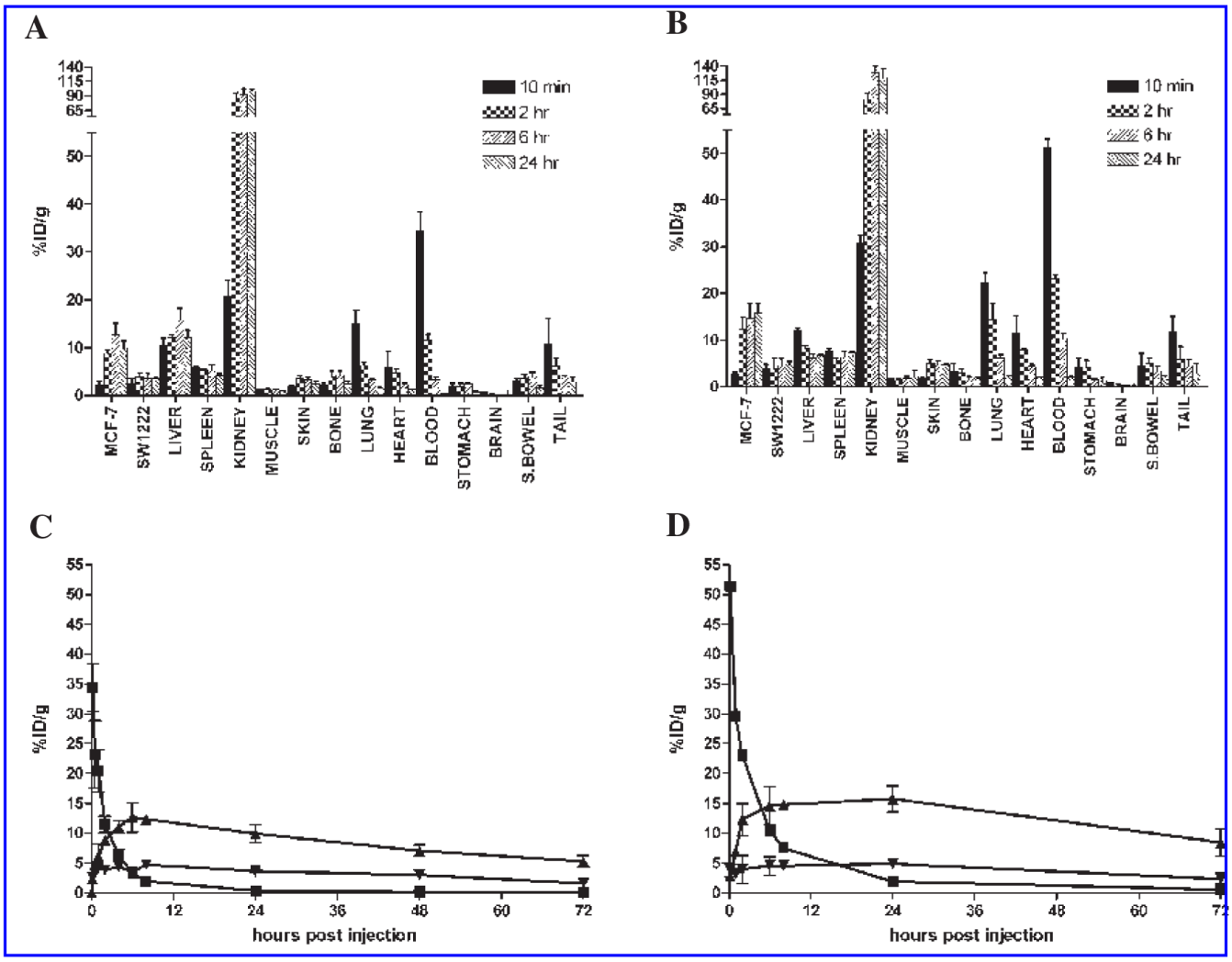

Figure 3.

(**A**) Biodistribution of ^{111}In-CHX-A″-DTPA hu3S193 multimer, and (**B**) ^{111}In-CHX-A″-DTPA hu3S193 F(ab′)$_2$ in normal tissues and tumors at 10 minutes and 2, 6, and at 24 hours postinjection. (**C**) Clearance and tumor localization of ^{111}In-CHX-A″-DTPA hu3S193 multimer and (**D**) ^{111}In-CHX-A″-DTPA hu3S193 F(ab″)$_2$ in blood (■), MCF-7 tumor (▲), and control SW1222 tumor (▼). Data are expressed as the mean ± standard deviation of the %ID/g for respective groups of $n = 5$.

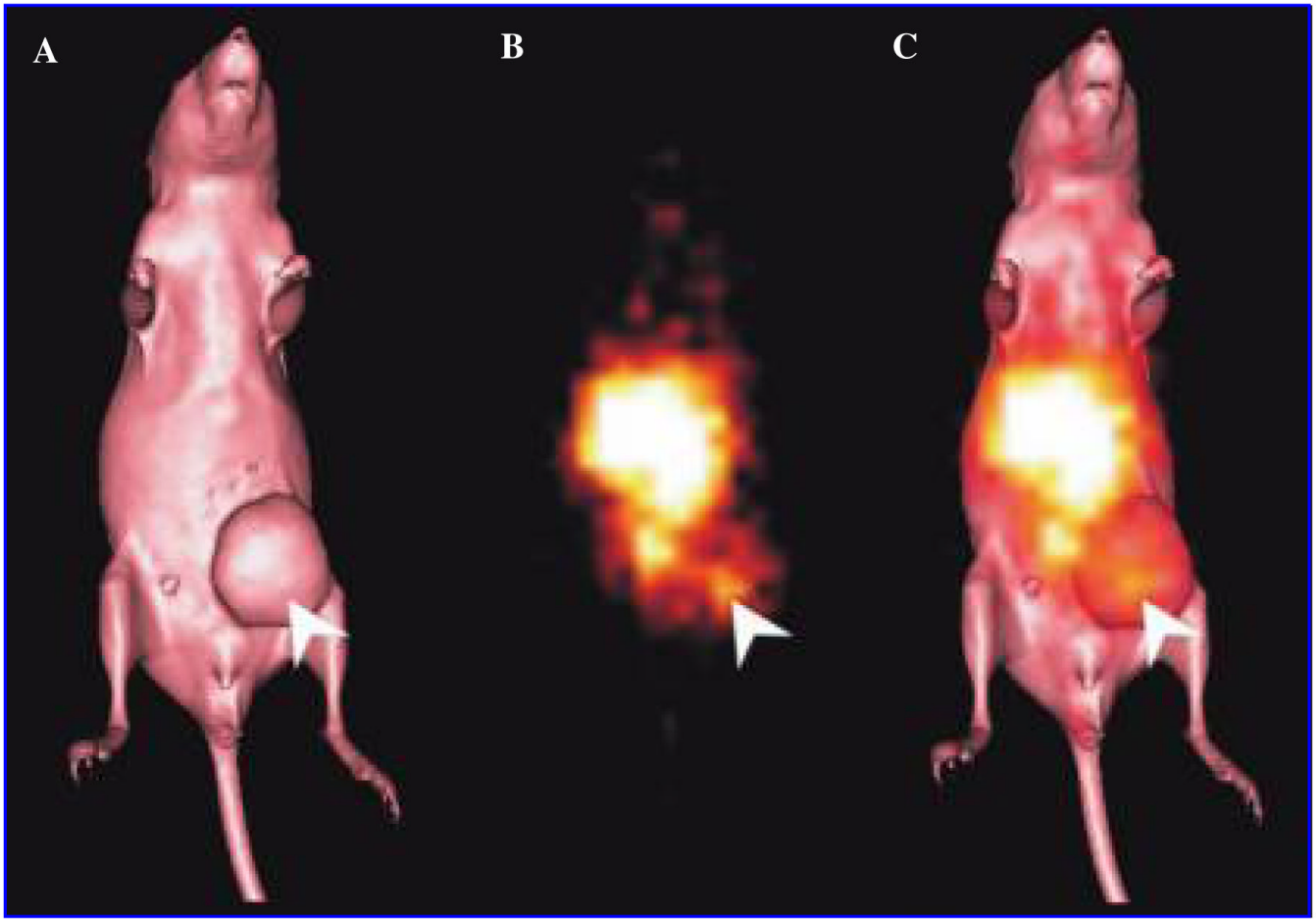

Figure 4.

(**A**) Surface-rendered computed tomography (CT) scan of a BALB/c nude mouse bearing a MCF-7 tumor on the left mammary line (right side of image). (**B**) Gamma-camera image obtained at 24 hours after an injection of the ^{111}In-CHX-A″-DTPA hu3S193 multimer. The tracer uptake observed in the center of the image corresponds to blood pool and kidney uptake. Localization of the hu3S193 multimer to the MCF-7 tumor is indicated by a white arrow. (**C**) Overlayed gamma-camera image and CT surface render showing the localization of the multimer in the tumor (arrow).

Table 1

Serum Stability of ^{111}In-CHX-A″DTPA hu3S193 Multimer and F(ab′)$_2$, and ^{111}In-CHX-A″DTPA huA33 F(ab′)$_2$ Constructs at 37°C

Time after incubation (hr)	Hu3S193 multimer %IR	Hu3S193 multimer % purity	Hu3S193 F(ab′)$_2$ %IR	Hu3S193 F(ab′)$_2$ % purity	HuA33 F(ab′)$_2$ %IR	HuA33 F(ab′)$_2$ % purity
0	76.1	>99	58.7	>99%	65.2	>99%
2	76.3	97.8	52.8	99%	67.2	99%
4	9.96	92.7	51.8	98.7	67.1	98.5
24	9.85	94.6	51.9	95.7	66.9	97.2

Percentage immunoreactivity (%IR) was determined by a single-point binding assay, whereas radiochemical purity (% purity) was determined by instant thin-layer chromatography.

Table 2

MCF-7 Tumor-to-Blood (T:B) Ratios and T:B Area Under Curve (AUC) Ratios for ^{111}In-CHX-A″-DTPA hu3S193 Multimer, diabody, and F(ab′)$_2$

Time point	Hu3S193 Multimer	*Hu3S193 Diabody*[a]	Hu3S193 F(ab′)$_2$
10 minutes	1:14.7	1:12	1:17.8
30 minutes	1:4.5	1:2	—
1 hour	1:3.2	1:2	1:4.2
2 hours	1:1.3	2:1	1:1.8
4 hours	1.3:1	5:1	—
6 hours	3.9:1	—	1.4:1
8 hours	6.4:1	20:1	2:1
24 hours	26.3:1	30:1	8.3:1
48 hours	46:1	40:1	—
72 hours	57:1	—	15.6:1
120 hours	46:1	—	—

	Hu3S193 Multimer	Hu3S193 Diabody	Hu3S193 F(ab′)$_2$
T:B AUC Ratio	6.28:1	6.32:1	3.31:1

[a] From Tahtis *et al.*[23]